PROCEEDINGS OF SCIENCE

Test-beam performance of a proton-irradiated, large-scale depleted monolithic active pixel sensors (DMAPS) in 150 nm CMOS technology

Lars Schall,[a,*] **Marlon Barbero,**[b] **Pierre Barrilon,**[b] **Christian Bespin,**[a] **Patrick Breugnon,**[b] **Ivan Caicedo,**[a] **Yavuz Degerli,**[c] **Jochen Dingfelder,**[a] **Tomasz Hemperek,**[a,d] **Toko Hirono,**[a,e] **Fabian Hügging,**[a] **Hans Krüger,**[a] **Patrick Pangaud,**[b] **Piotr Rymaszewski,**[a,d] **Philippe Schwemling,**[c] **Tianyang Wang,**[a,f] **Norbert Wermes**[a] **and Sinuo Zhang**[a]

[a] *Physikalisches Institut der Universität Bonn, Nußallee 12, Bonn, Germany*
[b] *CPPM, Aix Marseille University, 163 Avenue de Luminy, Marseille, France*
[c] *IRFU, CEA-Saclay, Batiment 141, Gif-sur-Yvette Cedex, France*
[d] *DECTRIS AG, Täfernweg 1, Baden-Dättwil, Switzerland*
[e] *Karlsruher Institut für Technologie, Kaiserstraße 12, Karlsruhe, Germany*
[f] *Zhangjiang National Laboratory, China*

E-mail: lars.schall@uni-bonn.de

The increasing availability of high-resistivity substrates and large biasing voltage capabilities in commercial CMOS processes encourage the use of depleted monolithic activate pixel sensors (DMAPS) in high-energy physics experiments. LF-Monopix2 is the latest iteration of a DMAPS development line designed in 150 nm LFoundry technology, which features a large scale (1×2) cm^2 chip size divided into (56×340) pixels with a pitch of (150×50) µm^2. Implementation of the full pixel electronic circuitry within a large charge collection node compromises the sensor's noise and power budget while assuring short drift distances and a homogeneous electric field in the sensing part of the detector that increase the radiation hardness. Laboratory characterization and beam test performance of 100 µm thick LF-Monopix2 sensors with backside processing and irradiated to 1×10^{15} n_{eq} cm^{-2} of NIEL fluence are presented.

The 32nd International Workshop on Vertex Detectors (VERTEX2023)
16-20 October 2023
Sestri Levante, Genova, Italy

*Speaker

PoS(VERTEX2023)043

1. Introduction

The technological advances and the increasing availability of high-resistivity substrates in commercial CMOS processes introduce new possibilities for the development of monolithic active pixel sensors (MAPS) for high-energy physics experiments [1]. MAPS unite readout electronics and sensor in one entity of silicon offering a lower material budget as well as less labor intensive and cheaper production in commercial foundries compared to the hybrid pixel detector concept. Depleted monolithic active pixel sensors (DMAPS) combine high-ohmic substrates ($\rho > 1\,\mathrm{k\Omega \cdot cm}$) with sufficiently large bias voltages, thus facilitating fast charge collection by drift through full depletion of the charge sensitive volume [2, 3]. This improves the radiation tolerance of the detector compared to conventional MAPS. Research an development of employing DMAPS in high-rate and high-radiation environments, such as those encountered in the ATLAS Inner Tracker upgrade [4], is ongoing. A typical design approach for DMAPS is to place the pixel electronics within a large collection electrode relative to the pixel pitch resulting in a homogeneous electric field and short drift distances over the entire pixel [5]. The latest prototype of the LF-Monopix DMAPS development line is a large-scale chip designed in 150 nm technology and high-resistivity substrate for compliance with the outer layer requirements of the ATLAS Inner Tracker upgrade [4, 6]. Latest laboratory characterization of threshold and noise as well as beam test results measured with proton-irradiated LF-Monopix2 sensors are presented in this contribution.

2. LF-Monopix2

LF-Monopix2 is the latest DMAPS prototype from the LF-Monopix development line designed in 150 nm LFoundry[1] CMOS technology. The chip has a size of $(1 \times 2)\,\mathrm{cm}^2$, i.e. full column length, of which 82 % is occupied by the pixel matrix with a pitch of $(50 \times 150)\,\mu\mathrm{m}^2$. It is read out using a synchronous column-drain readout architecture developed for the FE-I3 readout chip [7]. Exploiting its large collection electrode design approach, all in-pixel electronics is housed inside the collection node volume. Imporved shielding of the local, digital power domain addresses cross coupling from transients during digital activity into the collection electrode observed in its predecessor. The high biasing capabilities (breakdown voltage 450–500 V [8]) and large collection electrode of LF-Monopix2 facilitate short drift distances and a homogeneous electric field across a pixel. In return, the noise and rise time of the signal is compromised by the large sensor capacitance (250–300 fF) originating form the large collection electrode. Thus, more analog power is required to achieve the expected timing performance. Each pixel is equipped with a 4 −bit local threshold tuning DAC (TDAC) and a 6 −bit counter sampling the leading and trailing edge of discriminated signals with a 40 MHz clock. For testing purposes, the matrix is divided into multiple front-end variations, which are based on the best-performing front-end of its predecessor proven to be radiation-hard up to 100 Mrad total ionizing dose (TID) and $1 \times 10^{15}\,\mathrm{n_{eq}\,cm^{-2}}$ non-ionizing energy loss (NIEL) fluence [9, 10]. The front-end variants implemented in LF-Monopix2 differ by charge sensitive amplifier (CSA), local tuning circuitry, or feedback capacitance aiming to improve the timing performance [8]. LF-Monopix2 wafers have successfully been thinned-down to 100 µm and have been backside processed. Proton irradiated chips up to fluences of $2 \times 10^{15}\,\mathrm{n_{eq}\,cm^{-2}}$ from

[1] http://www.lfoundry.com/

Bonn and Birmingham irradiation sites [11, 12] are available. At the fluence of $2 \times 10^{15}\,\mathrm{n_{eq}\,cm^{-2}}$, this corresponds to radiation doses of 232 Mrad and 260 Mrad for the Bonn and Birmingham irradiation sites, respectively. All samples discussed in this contribution were not powered during the irradiation and were annealed for 80 min at 60 °C afterwards.

3. Characterization of irradiated LF-Monopix2

First, the general functionality of irradiated, thinned LF-Monopix2 chips measured in a controlled laboratory environment at −20 °C was confirmed. Figure 1 shows the leakage current as a function of bias voltage (I-V curves) before and after irradiation standardized to the total chip area of LF-Monopix2. The I-V curves were measured across the different irradiation steps, where only the measurement of the non-irradiated sensor was recorded at room temperature. An increase in leakage current of about $5\,\mu\mathrm{Acm^{-2}}$ per irradiation step of $1 \times 10^{15}\,\mathrm{n_{eq}\,cm^{-2}}$ was observed at 100 V reverse bias voltage. Up to 300 V, no breakdown was identified after irradiation, while higher voltages were deliberately avoided to prevent damage to the chip. Furthermore, no degradation in response and linearity of operational DACs of the front-end was observed after irradiation.

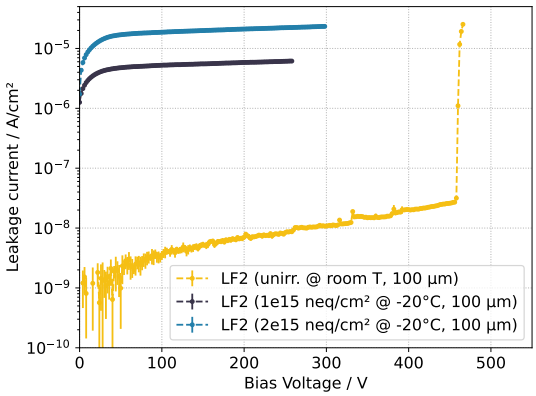

Figure 1: Leakage current of LF-Monopix2 at 0, 1 and $2 \times 10^{15}\,\mathrm{n_{eq}\,cm^{-2}}$ as a function of reversed bias voltage normalized to the total area of the chip.

Utilizing the digital in-pixel injection circuitry [8], a number of hits were injected into each pixel individually while continuously increasing the amount of injected charge. Given a smeared step function as pixel response, the threshold is defined as the charge at which 50 % of injected hits are detected by the pixel, whereas the smearing of the response is specified as equivalent noise charge (ENC). Figure 2 displays the tuned threshold and ENC distributions before and after irradiation to a fluence of $1 \times 10^{15}\,\mathrm{n_{eq}\,cm^{-2}}$ for the largest available front-end variant (in the following referred to as `Matrix 1`). The increase in leakage current after irradiation resulted in a 38 % higher mean ENC ($120\,\mathrm{e^-}$) due to the larger shot noise. Additionally, ~0.5 % of pixels had to be masked due to radiation damage. Nevertheless, a mean threshold of around $2\,\mathrm{ke^-}$ with a $112\,\mathrm{e^-}$ dispersion was achievable for $O(10\,000$ pixels).

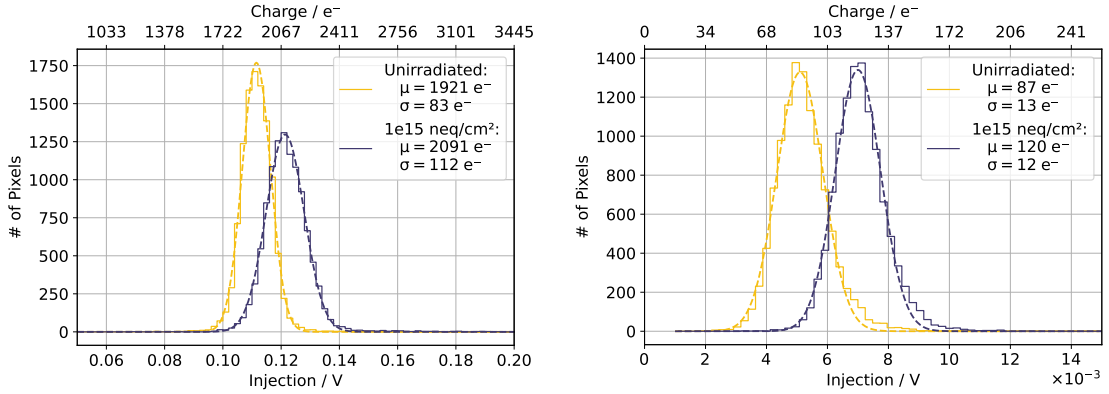

(a) **(b)**

Figure 2: Comparison of threshold (a) and ENC (b) distributions of LF-Monopix2 before and after irradiation to a fluence of 1×10^{15} n_{eq} cm^{-2} measured in a controlled laboratory environment at −20 °C.

3.1 Beam test measurements

Measurements in a 5 GeV electron beam have been performed at the DESY II test beam facility [13] using an EUDET-type beam telescope [14], a FE-I4 timing reference plane [15], and a scintillator synchronized through a trigger logic unit. A custom-made cooling setup employing dry ice and nitrogen was utilized to cool irradiated devices to a temperature of −20 °C during operation. All results shown in the following were measured with `Matrix 1` and set to a mean threshold of (2.0 ± 0.1) ke^- for a direct comparison of radiation effects. The most probable values (MPV) of the Landau-shaped calibrated charge spectra recorded for different bias voltages are shown in Figure 3(a) before and after irradiation. The corresponding depletion depths were derived assuming a charge creation of 71 $e^- \mu m^{-1}$ by 5 GeV electrons traversing 85 µm thick silicon (since 15 µm are occupied by non-sensitive metal and passivation layers [8]). Full depletion of the sensitive volume was reached at around 100 V after irradiation compared to 15 V in the non-irradiated case. As can be seen in Figure 3(b), the amount of collected charge correlates directly to the measured hit detection efficiency, where a total of (99.47 ± 0.10) % of hits were detected at full depletion. Utilizing the trigger-scintillator signal sampled in 640 MHz, the arrival time of a detected hit was measured in relation to its event. All events within a 25 ns window were considered to be *in-time*. The corresponding in-time efficiencies for various bias voltages are displayed in the same graph reaching (99.15 ± 0.10) % at 150 V. A general uncertainty of 0.1 % on all efficiencies is estimated for systematic errors during the measurement and in the analysis framework.

To achieve higher statistics and to study the performance within a pixel, a projection of the in-time efficiency results of the 1×10^{15} n_{eq} cm^{-2} irradiated sample onto a (2×2) pixel map is shown in Figure 4. Although a small drop to (97.79 ± 0.10) % in the pixel corners is visible, the efficiency within a 25 ns window remained above 97 % across the entire pixel corresponding to the initial design goal at the given irradiation level. This drop is expected since charge sharing is likely to happen for particles traversing the sensitive area in the corners of a pixel. The difference in beam test performance for the front-end variant of `Matrix 1` with a smaller feedback capacitance operated in full depletion at 150 V bias voltage and at a threshold of 2 ke^- is presented in Table 1.

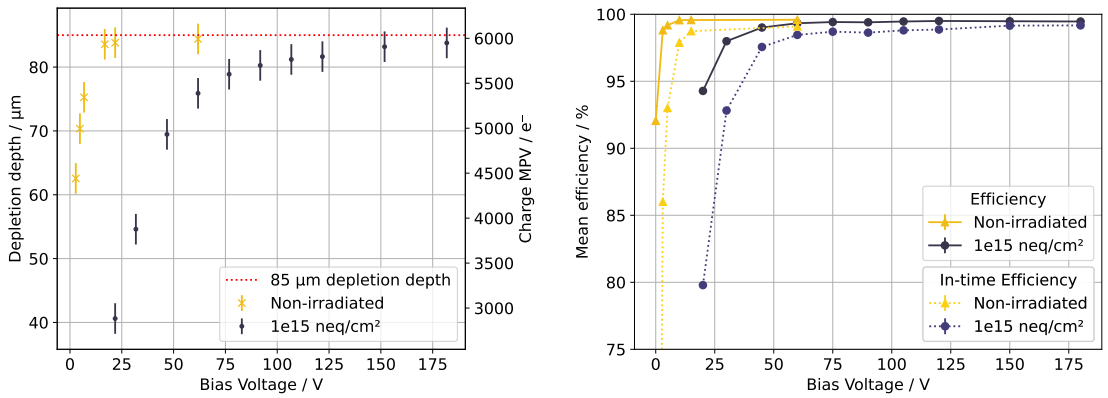

(a) **(b)**

Figure 3: Comparison of charge MPV and the derived depletion depth of a 5 GeV electron beam as a function of bias voltage before and after irradiation to $1 \times 10^{15}\,\mathrm{n_{eq}\,cm^{-2}}$ (a). The corresponding hit detection and in-time efficiencies are shown in (b). The improvement in efficiency for increasing bias voltages is visible until complete depletion of the sensitive volume is reached.

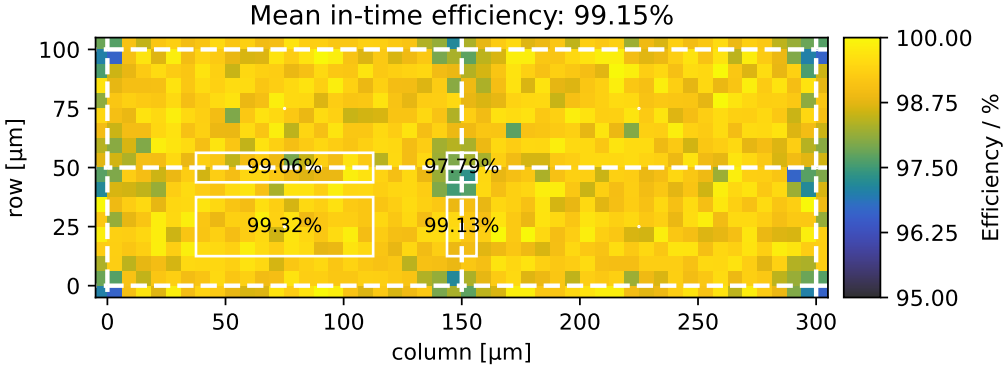

Figure 4: Measured in-time efficiency of `Matrix 1` projected onto a (2×2) pixel array of a $1\times10^{15}\,\mathrm{n_{eq}\,cm^{-2}}$ proton-irradiated LF-Monopix2 operated at 150 V bias voltage and 2 $\mathrm{ke^-}$ threshold. A small drop of in-time efficiency to (97.79 ± 0.10) % in the pixel corners is visible, as expected from charge sharing.

The reduction of the feedback capacitance $C_{Feedback}$ from 5 fF to 1.5 fF results in a larger gain [8] which increases the ratio of events within a 25 ns window and consequently the in-time efficiency. Comparing the results of `Matrix 1` to the hit detection efficiency of (99.59 ± 0.10) % with an in-time ratio of (99.43 ± 0.10) % measured for the same front-end variant with non-irradiated devices [8], no degradation in performance with respect to the error margin is observed.

4. Conclusion

Measurements of 100 µm thinned, backside processed LF-Monopix2 DMAPS have demonstrated very good performance after NIEL fluences of $1 \times 10^{15}\,\mathrm{n_{eq}\,cm^{-2}}$. Laboratory characterizations have proven the general functionality of the chip achieving an operational threshold close to 2 $\mathrm{ke^-}$ while observing a 38 % increase in ENC due to higher leakage current. Performance tests

$C_{Feedback}$	5 fF	1.5 fF
Hit-detection efficiency	(99.47 ± 0.10) %	(99.79 ± 0.10) %
In-time efficiency	(99.15 ± 0.10) %	(99.73 ± 0.10) %

Table 1: Comparison of hit detection and in-time efficiencies after irradiation to $1 \times 10^{15}\,n_{eq}\,cm^{-2}$ for different values of feedback capacitance $C_{Feedback}$ operated at $2\,ke^-$ threshold and 150 V bias voltage (fully depleted). The smaller feedback capacitance results in a larger gain and therefore an increase in in-time ratio.

in a 5 GeV electron beam have shown that full depletion of the sensitive volume is reached around 100 V after irradiation. Mean hit-detection and in-time efficiencies larger than 99 % are measured at full depletion and $2\,ke^-$ threshold with a small drop in the pixel corner, fulfilling the initial design goal of >97 % in-time efficiency after $1 \times 10^{15}\,n_{eq}\,cm^{-2}$ fluence. Comparing to non-irradiated LF-Monopix2 sensors, no significant degradation in beam test performance is observed. Encouraged by the good performance presented in this contribution, further characterization and beam tests with samples exposed to NIEL fluences higher than $1 \times 10^{15}\,n_{eq}\,cm^{-2}$ as well as dedicated TID irradiation studies are ongoing.

5. Acknowledgments

This project has received funding from the Deutsche Forschungsgemeinschaft DFG (grant WE 976/4-1), the German Federal Ministry of Education and Research BMBF (grant 05H15PDCA9), and the European Union's Horizon 2020 research and innovation programme under grant agreements no. 675587 (Maria Sklodowska-Curie ITN STREAM), 654168 (AIDA-2020), 101004761 (AIDAinnova), and 101057511 (EURO-LABS). The measurements leading to these results have partially been performed at the Test Beam Facility at DESY Hamburg (Germany), a member of the Helmholtz Association (HGF).

References

[1] R. Turchetta *et al.* "A monolithic active pixel sensor for charged particle tracking and imaging using standard VLSI CMOS technology," Nucl. Instrum. Meth. A **458** (2001), 677-689 doi:10.1016/S0168-9002(00)00893-7

[2] I. Peric "A novel monolithic pixelated particle detector implemented in high-voltage CMOS technology," Nucl. Instrum. Meth. A **582** (2007), 876-885 doi:10.1016/j.nima.2007.07.115

[3] M. Barbero *et al.* "Radiation hard DMAPS pixel sensors in 150 nm CMOS technology for operation at LHC," JINST **15** (2020) no.05, 05 doi:10.1088/1748-0221/15/05/P05013

[4] The ATLAS Collaboration "Technical Design Report for the ATLAS inner Tracker pixel detector" CERN-LHCC-2017-021, ATLAS-TDR-030 doi:10.17181/CERN.FOZZ.ZP3Q

[5] P. Rymazewski *et al.* "Development of depleted monolithic pixel sensors in 150 nm CMOS technology for the ATLAS Inner Tracker upgrade," PoS **TWEPP-17** (2018), 045 doi:10.22323/1.313.0045 [arXiv:1711.01233 [physics.ins-det]].

[6] J. Dingfelder *et al.* "Progress in DMAPS developments and first tests of the Monopix2 chips in 150 nm LFoundry and 180 nm TowerJazz technology," Nucl. Instrum. Meth. A **1034** (2022), 166747 doi:10.1016/j.nima.2022.166747

[7] I. Peric *et al.* "The FEI3 readout chip for the ATLAS pixel detector," Nucl. Instrum. Meth. A **565** (2006), 178-187 doi:10.1016/j.nima.2006.05.032

[8] I. Caicedo *et al.* "Improvement in the Design and Performance of Monopix2 Reticle-Scale DMAPS," JPS Conf. Proc. **Vertex2022** (In press)

[9] I. Caicedo *et al.* "Development and testing of a radiation-hard large-electrode DMAPS design in a 150 nm CMOS process," Nucl. Instrum. Meth. A **1040** (2022), 167224 doi:10.1016/j.nima.2022.167224

[10] T. Hirono *et al.* "Depleted fully monolithic active CMOS pixel sensors (DMAPS) in high resistivity 150 nm technology for LHC," Nucl. Instrum. Meth. A **924** (2019), 87-91 doi:10.1016/j.nima.2018.10.059

[11] D. Sauerland, R. Beck, J. Dingfelder, P. D. Eversheim and P. Wolf, "Proton Irradiation Site for High-Uniformity Radiation Hardness Tests of Silicon Detectors at the Bonn Isochronous Cyclotron," JACoW **CYCLOTRONS2022** (2023), MOBO03 doi:10.18429/JACoW-CYCLOTRONS2022-MOBO03

[12] P. Allport *et al.* "Recent results and experience with the Birmingham MC40 irradiation facility," JINST **12** (2017) no.03, C03075 doi:10.1088/1748-0221/12/03/C03075

[13] R. Diener *et al.* "The DESY II Test Beam Facility," Nucl. Instrum. Meth. A **922** (2019), 265-286 doi:10.1016/j.nima.2018.11.133

[14] H. Jansen *et al.* "Performance of the EUDET-type beam telescopes," EPJ Tech. Instrum. **3** (2016) no.1, 7 doi:10.1140/epjti/s40485-016-0033-2

[15] M. Garcia-Sciveres *et al.* "The FE-I4 pixel readout integrated circuit," Nucl. Instrum. Meth. A **636** (2011), S155-S159 doi:10.1016/j.nima.2010.04.101

PoS(VERTEX2023)043